J. Phys. Chem. A **2009,** *113,* 10343–10350 **10343**

On the Origin of Small Band Gaps in Alternating Thiophene−Thienopyrazine Oligomers

Bram P. Karsten,[†] Lucas Viani,[‡] Johannes Gierschner,[‡,§] Jérôme Cornil,[‡] and René A. J. Janssen[†,*]

Molecular Materials and Nanosystems, Eindhoven University of Technology, P.O. Box 513, NL-5600 MB Eindhoven, The Netherlands, Laboratory for Chemistry of Novel Materials, University of Mons-Hainaut, Place du Parc 20, B-7000 Mons, Belgium, and Madrid Institute of Advanced Studies, IMDEA-Nanoscience, UAM, Module C-IX, third Level, Av. Tómas y Valiente, 7 Campus Cantoblanco, E-28049 Madrid, Spain

Received: May 28, 2009; Revised Manuscript Received: July 15, 2009

We have studied experimentally and theoretically the optical and electrochemical properties of small band gap oligo(7,7′-bis(thiophen-2-yl)-5,5′-bisthieno[3,4-*b*]pyrazine)s with alternating blocks of bithiophene units and bisthienopyrazine units up to a total length of 16 units. The optical absorptions of the ground state, the triplet excited state, and the corresponding radical cation have been identified and shift to lower energy with increasing chain length. The optical absorption correlates well with quantum chemical calculations and the electrochemical band gap. We show that reduction of the band gap with chain length results from a significant rise of the HOMO level and a moderate reduction of the LUMO energy. Comparison of the chain length dependence of the transition energy at maximum absorption (E_{max}) and of the redox potentials with previously published data on oligothiophenes and related mixed thiophene−thienopyrazine oligomers shows that the reduction of E_{max} is more easily induced by increasing the number of thienopyrazine units than by extending the chain, mainly because thienopyrazine is both a better donor *and* a better acceptor than thiophene. Strong interactions between neighboring thienopyrazine units, with some possible admixing of quinoid character, are the main cause of the small band gap in these oligomers.

Introduction

Small band gap π-conjugated polymers are of profound interest for application in organic solar cells.[1] Their long wavelength absorption provides considerable overlap with the solar emission spectrum and enables increasing the photocurrent by converting a large fraction of photons into electrical energy. For single junction polymer solar cells the optimal optical band gap is presently considered to be about 1.4−1.5 eV,[2] while for multijunction cell architectures materials with even lower optical band gaps will be required.

Two different strategies exist toward designing and synthesizing small band gap polymers.[3] The first approach relies on creating polymers based on a single monomer unit that, after polymerization, endows the chain with an electronic structure where aromatic (A) and quinoid (Q) resonance structures are close in energy and bond length alternation is decreased or inverted. The classical example of this class, first described by Wudl et al., is poly(isothionaphthene), which features a band gap of about 1 eV due to an essentially quinoid ground state.[4] Another example in this class is poly(thienopyrazine), which has a similarly small optical band gap.[5] The second approach, first described by Havinga et al.[6] and further developed by Tanaka et al.,[7] is based on alternating electron-rich (donor) and electron-deficient (acceptor) monomer units along the chain that cause partial intramolecular charge transfer (ICT) and lead to small band gap semiconducting polymers. Using polysquaraines and polycroconaines, Havinga was able to lower the optical band gap down to ~0.5 eV. Presently, the large majority of small band gap polymers developed for solar cell applications is based on this donor−acceptor (DA) approach.[1] Frequently, small oligothiophene derivatives with two to four units are used as the electron-rich donor unit with the complementary electron-deficient acceptor units being an aromatic nitrogen heterocyclic system, such as quinoxaline, 1,3,2-benzothiadiazole, or thieno[3,4-*b*]pyrazine.[1] Kertesz et al., however, have pointed out on the basis of theoretical considerations that alternating donor−acceptor (DA) copolymers might also be considered as alternating aromatic−quinoid (AQ) copolymers, reflecting that the A units tend to be aromatic in poly-A and the Q units quinoid in poly-Q.[3c]

Virtually all small band gap polymers reported to date have a single acceptor unit alternating with more extended donor segments along the chain. In this work, we present the synthesis and optical properties of a new series of oligomers comprising *two* electron-rich thiophene (T) units alternating with *two* electron-deficient thienopyrazine (TP) units. These $(\mathrm{T{-}TP_2{-}T})_n$ oligomers are homologues of the $(\mathrm{T{-}TP{-}T})_n$ and $\mathrm{T{-}TP}_n\mathrm{{-}T}$ series[8,9] that we described recently and evaluated the effect of extra thienopyrazine units in the backbone. Comparison of the optical and electrochemical signatures of the two series at the experimental and theoretical levels reveals that for these T−TP oligomers donor−acceptor interactions are *not* the principal reason for the small band gap. The experiments and calculations reveal that the TP unit is both a better donor *and* a better acceptor than T. Hence, for a fixed number of repeat units ($n + m$), the band gap of a $\mathrm{T}_n\mathrm{TP}_m$ oligomer decreases when n decreases in favor of m.

---

* To whom correspondence should be addressed. E-mail: r.a.j.janssen@tue.nl.

[†] Eindhoven University of Technology.

[‡] University of Mons-Hainaut.

[§] Madrid Institute of Advanced Studies.

10.1021/jp9050148 CCC: $40.75

Experimental Methods

General Methods. ^{1}H NMR and ^{13}C NMR spectra were recorded on a 400 MHz NMR (Varian Mercury, 400 MHz for ^{1}H NMR and 100 MHz for ^{13}C NMR), and chemical shifts are reported in ppm downfield from tetramethylsilane (TMS). IR spectra were recorded on a Perkin-Elmer 1600 FT-IR. Matrix-assisted laser desorption ionization time-of-flight (MALDI-TOF) mass spectrometry has been performed on a PerSeptive Biosystems Voyager-DE PRO spectrometer. UV/vis spectra were recorded on a Perkin-Elmer Lambda 900 UV/vis/NIR spectrometer. Recycling GPC was performed on a LC system equipped with JAIGEL 2H and JAIGEL 2.5H columns and a UV-detector, using a preparative flow cell (path length 0.5 mm). The eluent was chloroform at 3.5 mL/min, the injection volume was 2 mL. Cyclic voltammograms were recorded in an inert atmosphere with 0.1 M tetrabutylammonium hexafluorophosphate (TBAPF$_6$) in ODCB as supporting electrolyte. The working electrode was a platinum disk (0.2 cm^2) and the counter electrode was a silver electrode. The samples were measured using an Ag/AgCl reference electrode with Fc/Fc$^+$ as an internal standard using a μAutolab II with a PGSTAT30 potentiostat at a scan speed of 200 mV/s. PIA spectra were recorded by exciting with a mechanically modulated cw Ar ion laser ($\lambda = 351$ and 364 nm, 275 Hz) pump beam and monitoring the resulting change in transmission of a tungsten−halogen probe light through the sample (ΔT) with a phase-sensitive lock-in amplifier after dispersion by a grating monochromator and detection, using Si, InGaAs, and cooled InSb detectors. The pump power incident on the sample was typically 25 mW with a beam diameter of 2 mm. The PIA ($\Delta T/T$) was corrected for the photoluminescence, which was recorded in a separate experiment. Photoinduced absorption spectra and photoluminescence spectra were recorded with the pump beam in a direction almost parallel to the direction of the probe beam. The solutions were studied in a 1 mm near-IR grade quartz cell at room temperature.

Theoretical Calculations. Quantum chemical calculations were performed to investigate the electronic and optical properties of the oligomers at a theoretical level. The quantum chemical methods used in this work have been described and motivated in detail previously.[8] Briefly, the method entails the following approach and approximations: (1) The conjugated backbone was imposed to be planar and the long alkyl side chains were replaced by methyl groups to minimize the computational efforts. (2) The ground-state molecular geometries were optimized by the MNDO (modified neglect of differential overlap) method, as implemented in the AMPAC package.[10] (3) The electronic structure was calculated with the INDO (intermediate neglect of differential overlap) method, as parametrized by Zerner and co-workers, and using the Ohno−Klopman potential.[11] (4) The INDO results were coupled to a single configuration interaction (SCI) scheme including all $\pi \rightarrow \pi^*$ transitions to calculate the vertical transition energy ($E_{\text{ver}}^{\text{cal}}$) between the ground and lowest excited states ($S_1 \leftarrow S_0$).[12]

Materials. Solvents were purchased from Biosolve and used without further purification, unless stated otherwise. THF was distilled over 4 Å molecular sieves before use. Chemicals were purchased from Acros or Aldrich and used without purification. The synthesis of monomer (**1**) was published earlier.[9] Oxygen- and moisture-sensitive reactions were performed under an argon atmosphere.

Oligo(2,2′,3,3′-tetrakis(2-ethylhexyl)-7,7′-bis(3-octylthiophen-2-yl)-5,5′-bisthieno[3,4-*b*]pyrazine) (4, *n* = 2, 3, 4). 2,2′,3,3′-Tetrakis(2-ethylhexyl)-7,7′-bis(3-octylthiophen-2-yl)-5,5′-bisthieno[3,4-*b*]pyrazine (**1**) (505 mg, 0.46 mmol) was dissolved in THF (20 mL). *N*-Bromosuccinimide (89 mg, 0.50 mmol) was added at 0 °C, in the absence of light. The mixture was stirred overnight, while being warmed to room temperature. Diethyl ether (100 mL) was added and the mixture was washed with water (3 × 50 mL) and saturated NaCl (2 × 50 mL). The organic phase was dried with MgSO$_4$ and the solvent was evaporated. The resulting monomer mixture (**2** + **3**) was brought under an argon atmosphere. Ni(COD)$_2$ (280 mg, 1.02 mmol) and 2,2′-bipyridyl (149 mg, 0.95 mmol) were dissolved in toluene (15 mL) and stirred 0.5 h at 80 °C. The Ni(COD)$_2$/bipyridyl mixture was added to the monomer mixture and stirred at 80 °C for 21 h. A 1:1:1 methanol/acetone/0.1 M HCl mixture (200 mL) was added and the mixture was stirred for 1 h. The product was extracted with chloroform (2 × 100 mL), EDTA (disodium salt) (1.6 g) was added, and the mixture was stirred for 3 h. The mixture was washed with water (3 × 200 mL), concentrated, and precipitated in methanol (300 mL). The crude product mixture was filtered into a Soxhlet thimble and fractionated by Soxhlet extraction with methanol, hexane, and dichloromethane. The hexane and dichloromethane extracts were separated by recycling GPC, yielding pure oligomers. Yields: monomer, 10 mg; dimer, 80 mg; trimer, 68 mg; tetramer, 21 mg.

Dimer. ^{1}H NMR (400 MHz) δ (ppm): 7.38 (s, 2p, Ar-*H*), 7.19 (s, 2p, Ar-*H*), 7.04 (s, 2p, Ar-*H*), 3.10 (m, 8p, $-CH_2C_7H_{15}$), 3.00−2.86 (m, 16p, $-CH_2CH(C_4H_9)(C_2H_5)$), 2.45−2.20 (m, 8p, $-CH_2CH(C_4H_9)(C_2H_5)$), 1.90−1.72 (m, 8p, $-CH_2CH_2C_6H_{13}$), 1.62−1.18 (m, 104p, $-CH_2-$), 1.07−0.81 (m, 60p, $-CH_3$). IR (cm^{-1}): 2956, 2923, 2855, 1486, 1440, 1377, 1352, 1239, 1181, 1138, 1121, 826, 802, 725, 701. MALDI-TOF-MS *m/z* (intensity, %): 2211.11 (60), 2212.10 (95), 2213.10 (100), 2214.09 (80), 2215.08 (50), 2216.08 (30), 2217.07 (15).

Trimer. ^{1}H NMR (400 MHz) δ (ppm): 7.38 (d, $J = 5.1$ Hz, 2p, Ar-*H*), 7.19 (s, 4p, Ar-*H*), 7.04 (d, $J = 5.2$ Hz, 2p, Ar-*H*), 3.16−3.05 (m, 12p, $-CH_2C_7H_{15}$), 3.02−2.87 (m, 24p, $-CH_2CH(C_4H_9)(C_2H_5)$), 2.45−2.20 (m, 12p, $-CH_2CH(C_4H_9)(C_2H_5)$), 1.92−1.72 (m, 12p, $-CH_2CH_2C_6H_{13}$), 1.60−1.20 (m, 156p, $-CH_2-$), 1.07−0.80 (m, 90p, $-CH_3$). IR (cm^{-1}): 2956, 2923, 2855, 1485, 1457, 1440, 1377, 1351, 1247, 1181, 1137, 1121, 825, 802, 724, 699. MALDI-TOF-MS *m/z* (intensity, %): 3315.56 (35), 3316.55 (70), 3317.55 (95), 3318.55 (100), 3319.54 (85), 3320.55 (60), 3321.55 (45), 3322.57 (30).

Tetramer. ^{1}H NMR (400 MHz) δ (ppm): 7.38 (d, $J = 5.0$ Hz, 2p, Ar-*H*), 7.19 (s, 6p, Ar-*H*), 7.04 (d, $J = 4.9$ Hz, 2p, Ar-*H*), 3.17−3.06 (m, 16p, $-CH_2C_7H_{15}$), 3.02−2.86 (m, 32p, $-CH_2CH(C_4H_9)(C_2H_5)$), 2.46−2.20 (m, 16p, $-CH_2CH(C_4H_9)(C_2H_5)$), 1.92−1.73 (m, 16p, $-CH_2CH_2C_6H_{13}$), 1.64−1.20 (m, 208p, $-CH_2-$), 1.07−0.80 (m, 120p, $-CH_3$). IR (cm^{-1}): 2956, 2923, 2854, 1485, 1457, 1440, 1377, 1350, 1250, 1181, 1137, 1121, 1097, 825, 802, 724. MALDI-TOF-MS *m/z*: 4425.43.

Results and Discussion

Synthesis. (T−TP$_2$−T)$_n$ oligomers of different length were synthesized in a one-step procedure outlined in Scheme 1 and subsequently separated using recycling GPC. The synthesis of the T−TP$_2$−T monomer (**1**) has been described in ref 9. Partial bromination using NBS yielded a mixture of monobrominated and dibrominated compounds (**2** and **3**). This mixture was then subjected to a nickel(0)-mediated Yamamoto oligomerization[13] in which **2** acts as a chain stopper to provide a mixture of shorter oligomers (**4**) of various lengths. After a first separation of this mixture by Soxhlet extraction, we used recycling GPC to obtain the oligomers in pure form. Recycling GPC is a preparative-scale GPC technique, in which the eluted products are fed back

SCHEME 1: Synthesis of the Oligomers of 2,2′,3,3′-Tetrakis(2-ethylhexyl)-7,7′-bis(3-octylthiophen-2-yl)-5,5′-bithieno-[3,4-*b*]pyrazine

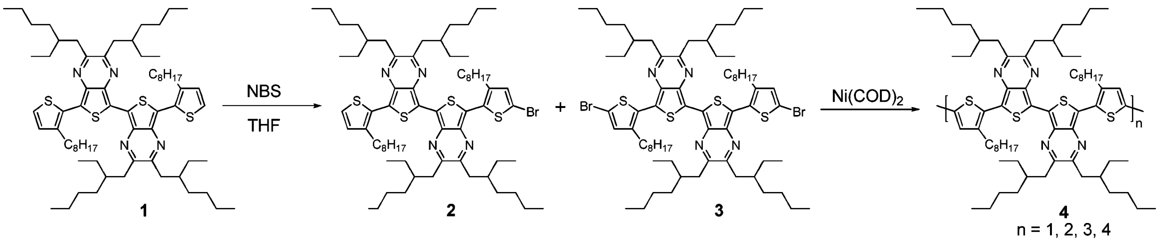

TABLE 1: UV/Vis/NIR Absorption Data in Toluene and Onset of Redox Potentials (E_{ox} and E_{red}, vs Fc/Fc$^+$) in ODCB for the Oligomers[a]

	neutral oligomers									radical cations	
n	λ_{max} (nm)	E_{max} (eV)	λ_{onset} (nm)	E_g^{opt} (eV)	E_{ox} (V)	E_{red} (V)	E_g^{cv} (V)	$E_g^{cv} - E_g^{opt}$ (eV)	$T_n \leftarrow T_1$ (eV)	$D_2 \leftarrow D_0$ (eV)	$D_1 \leftarrow D_0$ (eV)
1	629	1.97	756	1.64	−0.08	−1.78	1.70	0.06		1.58	0.96
2	736	1.68	882	1.41	−0.26	−1.69	1.43	0.02	1.22	0.93	0.52
3	775	1.60	948	1.31	−0.35	−1.68	1.33	0.02	1.18	0.83	0.48
4	792	1.57	975	1.27	−0.39	−1.67	1.28	0.01	1.12	0.83	0.46

[a] $T_n \leftarrow T_1$ absorption in toluene. $D_2 \leftarrow D_0$ and $D_1 \leftarrow D_0$ absorptions of the radical cations in benzonitrile.

into the column, thereby virtually creating a GPC column of very long length, without having the problem of a very high pressure drop. The consecutive oligomers were collected during the repetitive cycles by temporarily switching the recycle valve to the collect position. This technique provides monodisperse, pure oligomers ($n = 1-4$) as evidenced from MALDI-TOF mass spectrometry, NMR, and FT-IR. The longest oligomer that was isolated in pure form ($n = 4$) has 16 units along the chain.

Optical and Electrochemical Properties of the Neutral Oligomers. The $\pi-\pi^*$ optical absorption of the $(T-TP_2-T)_n$ oligomers shifts to longer wavelengths when n increases from 1 to 4 (Table 1, Figure 1a). Already for $n = 1$ the onset of absorption (λ_{onset}) is outside the visible region of the spectrum. The energies of maximum absorption (E_{max}) and the onsets (E_g^{opt}) in solution are collected in Table 1.

The optical band gap (E_g^{opt}) of the $(T-TP_2-T)_n$ oligomers is plotted versus $1/n$ in Figure 2. To describe the dispersion of the optical band gap with chain length we have used an empirical relation that accounts for the leveling off of the curve at longer chain lengths.[14]

$$E(n) = E_\infty + (E_1 - E_\infty)\exp[-a(n-1)] \qquad (1)$$

In this relation, E_1 and E_∞ are the excitation energies for the monomer and the (infinitely long) polymer, n is the number of repeat units, and a is a parameter that describes how fast $E(n)$ saturates to E_∞. Fitting the optical band gaps E_g^{opt} of the oligomers to eq 1 yields $E_\infty = 1.24$, $E_1 = 1.64$ eV, and $a = 0.85$. From the value of a, it follows that 99% of the band gap reduction will be completed at about six repeat units, similar to the conversion of the $(T-TP-T)_n$ series of oligomers.

The cyclic voltammograms recorded for each of the four $(T-TP_2-T)_n$ oligomers dissolved in ODCB (Figure 1b) reveal one or more quasireversible oxidation and reduction wave. Oxidation of the oligomers occurs at rather low potentials, even below 0 V vs Fc/Fc$^+$. Peak potentials of the successive oxidation and reduction waves are summarized in Table 2. From the relative intensities of the oxidation and reduction waves in the voltammogram, it can be seen that, for the longer oligomers ($n > 1$), the first reduction wave corresponds to a multielectronic process. The same holds for the first oxidation wave when $n > 2$.

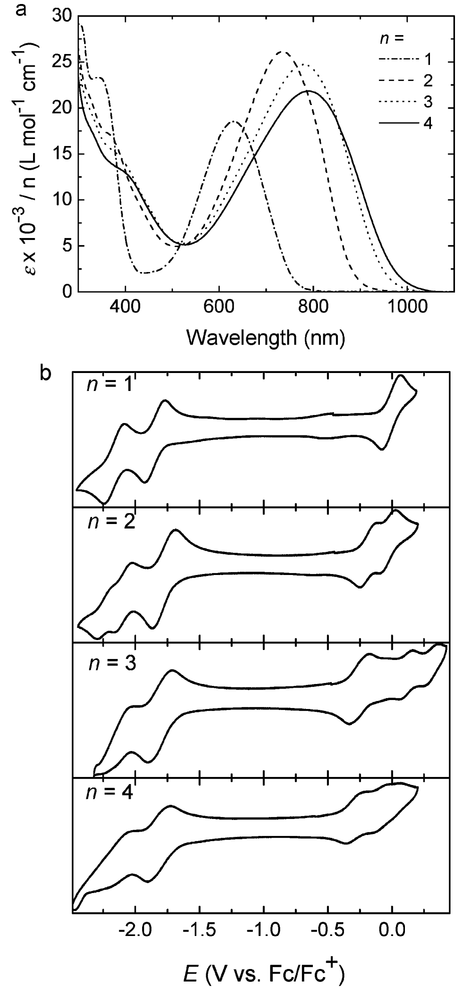

Figure 1. (a) UV/vis/NIR absorption spectra of the $(T-TP_2-T)_n$ oligomers in toluene, given in molar extinction coefficients per repeating unit. (b) Cyclic voltammograms of the oligomers in ODCB.

The potentials at the onsets of the redox waves (E_{ox} and E_{red}) have been used to estimate the electrochemical band gap ($E_g^{cv} = E_{ox} - E_{red}$) (Table 1). These onsets were determined as the

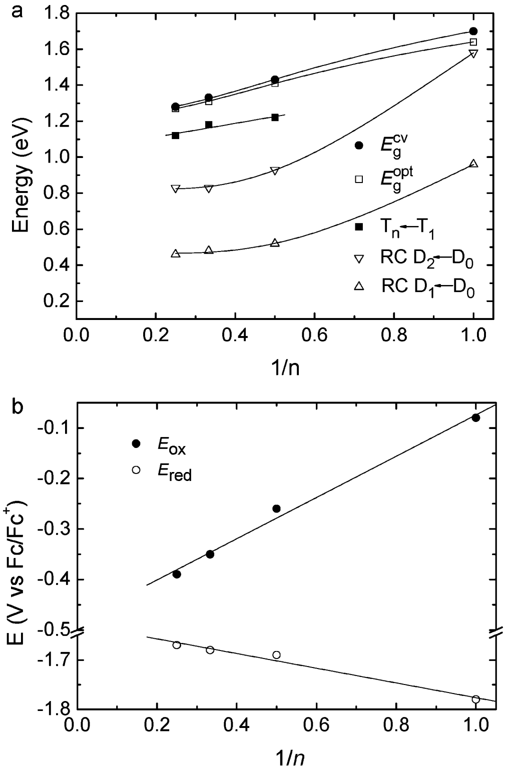

Figure 2. (a) Chain length dependence of the energies for the optical and electrochemical band gap, the triplet $T_n \leftarrow T_1$ absorption, and the radical cation absorptions ($D_1 \leftarrow D_0$ and $D_2 \leftarrow D_0$) vs reciprocal chain length (1/*n*) for the (T−TP$_2$−T)$_n$ oligomers. (b) Onsets of oxidation and reduction vs 1/*n*. Fits of the data are to eq 1 for the band gaps and the radical cation absorption; other data are fitted to a linear relation with 1/*n*.

crossing of the tangents to the baseline and the redox wave in its inflection point. The accuracy of this method is ca. 0.01 V. The electrochemical band gap, E_g^{cv}, is slightly larger than the optical band gap, E_g^{opt}, but decreases in a similar fashion with chain length. Apart from experimental uncertainties, the difference between E_g^{opt} and E_g^{cv} reflects the fact that free ions are created and solvated in the electrochemical experiment rather than a neutral exciton under optical excitation. E_g^{opt} and E_g^{cv} increase almost linearly with the reciprocal chain length (1/*n*) (Figure 2a). Figure 2b shows that the oxidation and reduction potentials change almost linearly with 1/*n* in the range studied. Figure 2b shows furthermore that the decrease in the electrochemical band gap is mainly (for ~75%) due to a lowering of the oxidation potential because the change of reduction potentials with chain length is much less pronounced. The same has previously been observed for the (T−TP−T)$_n$ oligomers that contain only one TP unit per two T units. Compared to (T−TP−T)$_n$, the (T−TP$_2$−T)$_n$ series has a lower oxidation and lower reduction potential. This is maybe somewhat unexpected because lowering of the oxidation potential, with increasing number of TP acceptor units, implies that they also have significant donor characteristics; this is actually supported by the delocalized character of the HOMO level suggested by the calculations (vide infra). On the other hand, the interaction between the acceptor parts of the molecule is less pronounced due to their localized character.

Triplet States of the Neutral Oligomers. Direct excitation of the (T−TP$_2$−T)$_n$ oligomers in toluene did not produce any detectable amount of the corresponding triplet states using near steady-state photoinduced absorption (PIA). The triplet states for $n > 1$, however, could readily be populated and studied using a fullerene derivative ([6,6]-phenyl-C$_{61}$-butyric acid methyl ester, PCBM) as triplet sensitizer.[15] PCBM has a very high quantum yield for triplet formation after absorbing a photon. In a toluene solution the triplet excited PCBM can transfer its energy to the (T−TP$_2$−T)$_n$ oligomer, producing the corresponding triplet state. The PIA spectra recorded for mixtures of the oligomer (0.1 mM) and PCBM (0.4 mM) in toluene with excitation at 351 and 364 nm are shown in Figure 3. Although the signals are rather weak, the $T_n \leftarrow T_1$ absorption peak clearly shifts to lower energy with increasing *n*. For the monomer, the triplet state is not observed in this experiment. Instead, for $n = 1$ the PIA spectrum is characteristic for that of the triplet state of PCBM with a peak at 1.78 and a shoulder at 1.52 eV.[16] This signal can also be observed in the PIA spectra of the other oligomers and overlaps with the bleaching band of the ground state absorption. The $T_n \leftarrow T_1$ absorption maximum for the three longer oligomers ($n = 2-4$) is plotted versus 1/*n* in Figure 2a. Because the data is limited to only three points, only a linear fit has been made, which suggests that the $T_n \leftarrow T_1$ absorption for the polymer would be located around 1.05 eV.

Radical Cations of the Oligomers. When using PCBM as a triplet sensitizer in PIA experiments, the polarity of the solvent is an important parameter for the outcome of the reaction. As shown in the paragraph above, in an apolar solvent like toluene ($\varepsilon_r = 2.4$) the T$_1$ state of PCBM can transfer its triplet excitation energy to the oligomer. However, as PCBM is also an electron acceptor in the triplet state, the same experiment can also result in an electron transfer reaction between PCBM and the oligomer, producing the radical cation of the latter and the PCBM radical anion. Electron transfer is favored in more polar solvents (e.g., in benzonitrile, $\varepsilon_r = 25.9$), because the solvent may stabilize the charge-separated state solvation and screening of the ions. The discrimination between the two processes can be described by the Weller equation in terms of the free energy for charge separation (ΔG_{CS}):[17]

$$\Delta G_{CS} = e[E_{ox}(D) - E_{red}(A)] - E_{00} - \frac{e^2}{4\pi\varepsilon_0\varepsilon_s R_{cc}} - \frac{e^2}{8\pi\varepsilon_0}\left(\frac{1}{r^+} + \frac{1}{r^-}\right)\left(\frac{1}{\varepsilon_{ref}} - \frac{1}{\varepsilon_s}\right) \quad (2)$$

In this equation E_{ox}(D) and E_{red}(A) represent the redox potentials of the donor (oligomer) and acceptor (PCBM, E_{red}(A)

TABLE 2: Anodic (E_{pa}) and Cathodic (E_{pc}) Peak Potentials of the Successive Redox Waves (V vs Fc/Fc$^+$) in ODCB for the Oligomers

	oxidation						reduction					
n	E_{pa}	E_{pc}	E_{pa}	E_{pc}	E_{pa}	E_{pc}	E_{pa}	E_{pc}	E_{pa}	E_{pc}	E_{pa}	E_{pc}
1	0.07	−0.08					−1.77	−1.93	−2.09	−2.24		
2	−0.12	−0.25	0.03	−0.09			−1.69	−1.87	−2.03	−2.16		−2.30
3	−0.18	−0.33	0.16	0.07	0.36	0.25	−1.71	−1.90				
4	−0.21	−0.35					−1.73	−1.90				

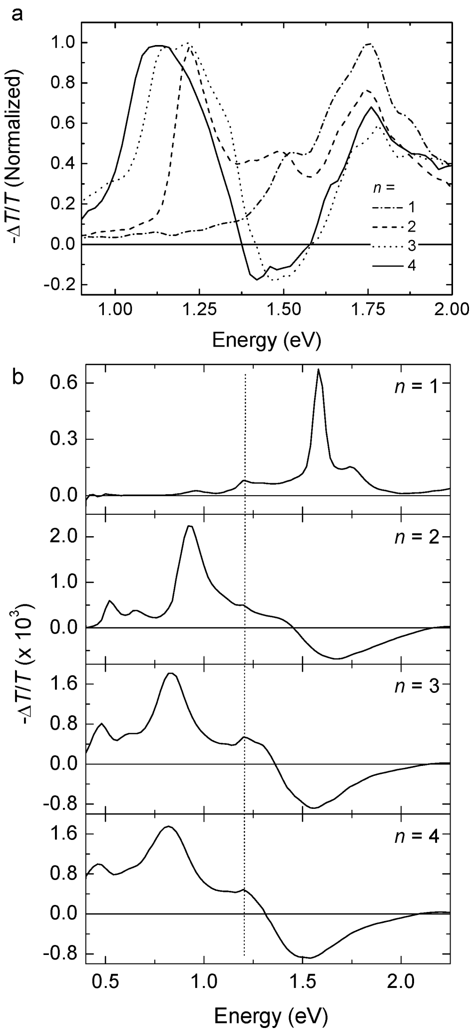

Figure 3. PIA spectra of the mixtures of the $(T-TP_2-T)_n$ oligomers (0.1 mM) and PCBM (0.4 mM) dissolved in toluene (a) and benzonitrile (b), recorded at room temperature with excitation at 351 and 364 nm. The vertical dotted line in panel b indicates the position of the PCBM radical anion.

$= -1.08$ V vs Fc/Fc$^+$),[18] E_{00} is the energy of the photoexcited state (1.50 eV for the triplet level of fullerene derivatives like PCBM[19]), and R_{cc} is the center to center distance of the positive and negative charges (set to infinity for intermolecular charge transfer), r^+ and r^- are the radii of the positive and negative ions, and ε_{ref} and ε_s are the relative permittivities of the reference solvent (used to measure oxidation and reduction potentials) and the solvent in which is measured. r^- is calculated in literature to be 5.6 Å for C_{60}, based on the density of C_{60}.[19] r^+ can be estimated using a similar approach, using a density of 1.5 g/cm^3, the value for unsubstituted terthiophene.[20] This calculation for the different oligomers yields the values given in Table 3. On the basis of these data, we expect triplet absorptions in toluene, as observed (Figure 3a), but photoinduced electron transfer in benzonitrile (Figure 3b).

The PIA spectra of $(T-TP_2-T)_n-$PCBM mixtures dissolved in benzonitrile (Figure 3b) show two absorption peaks due the radical cation of the oligomer and a bleaching band at of the neutral compound at higher energy. In each of the spectra a weak band at 1.20 eV signifies the presence of the PCBM radical anion.[15] The two absorption bands of the doublet-state radical cations correspond to dipole-allowed $D_1 \leftarrow D_0$ and $D_2 \leftarrow D_0$ transitions and result from electron excitations from HOMO → SOMO (singly occupied molecular orbital) and SOMO → LUMO. The transition energies of these bands (Table 1, Figure 2) have been fitted to eq 1 to give $E_\infty = 0.82$, $E_1 = 1.58$, and $a = 1.97$ for the $D_2 \leftarrow D_0$ band and $E_\infty = 0.47$, $E_1 = 0.96$, and $a = 2.18$ for the $D_1 \leftarrow D_0$ band. The high values for a indicate a much faster saturation of the transition energies for the radical cation than for the absorption bands of the neutral molecule. Hence, the optical transitions are likely to be more localized in the radical cation than in the neutral molecule.

TABLE 3: Free Energies for Charge Separation Based on Eq 2

n	E_{ox} (ODCB) (V vs Fc/Fc+)	r^+ (Å)	ΔG_{CS} (eV) toluene	ΔG_{CS} (eV) benzonitrile
1	0	4.86	0.47	−0.59
2	−0.18	6.13	0.19	−0.75
3	−0.25	7.01	0.07	−0.81
4	−0.28	7.72	0.01	−0.83

Chain Length Dependence in Related Systems. To obtain more insight in the effects that determine the band gap in thiophene−thieno[3,4-*b*]pyrazine-based donor−acceptor systems, the chain length dependence of the maximum of absorption, E_{max}, and the redox potentials of the $(T-TP_2-T)_n$ series can be compared with data for related systems T_n,[21,22] $(T-TP-T)_n$,[8] $T-TP_3-T$,[9] poly-T_n, and poly-TP_n[5c] already published. To be able to compare these different systems, we use the total number of rings N in the main chain as the common parameter. Figure 4 shows E_{max}, E_{ox}, and E_{red} versus $1/N$, as well as the calculated vertical transition energies E_{vert} and the calculated HOMO and LUMO levels for the different series (Table 4). There is a fairly good agreement between the experimental E_{max} and calculated optical transitions E_{vert}, especially for the evolution with chain length N. Differences in the absolute positions might arise from the thermal population of torsion modes, which are neglected in the calculations,[12] and from the neglect of solvent effects. The large HOMO−LUMO gaps provided by the INDO method are due to a conjunction between the inherent parametrization of ZINDO, the assumption of Koopmans' theorem in the calculations, and the neglect of solvent effects. In any case, the evolution of the energies of the occupied or unoccupied levels among the different series is reliable with this theoretical approach.

From Figure 4 it is clear that the curvature of E_{max} (and its calculated equivalent E_{vert}) with $1/N$ is virtually identical for simple oligothiophenes (T_n) and for alternating $(T-TP-T)_n$ and $(T-TP_2-T)_n$ donor−acceptor systems. On the other hand, when comparing the $T-TP_n-T$ monomers ($n = 0-3$) in the graphs (dashed line) it is evident that increasing the amount of thienopyrazine in the acceptor blocks causes a very strong reduction of E_{max}. The influence of adding *one* extra thienopyrazine unit to the repeat unit is almost as large as the total reduction in E_{max} upon going from one repeat unit to the polymer. This is further illustrated in Figure 5,which shows E_{max} and E_g^{opt} for the polymers as a function of the fraction of TP units in the chain. The proportionality is much stronger than a simple linear relation such that already a fraction of ∼20% thienopyrazine units is responsible for half the band gap reduction.

If the band gap reduction with increasing acceptor block size would be purely based on donor−acceptor effects, localization of both HOMO and LUMO on the respective donor and acceptor units will inevitably lead to smaller orbital coefficients on the atoms connecting the different units when the donor or acceptor blocks become larger. This effect would lead to a reduction of the chain length dependence and significantly reduce the slope

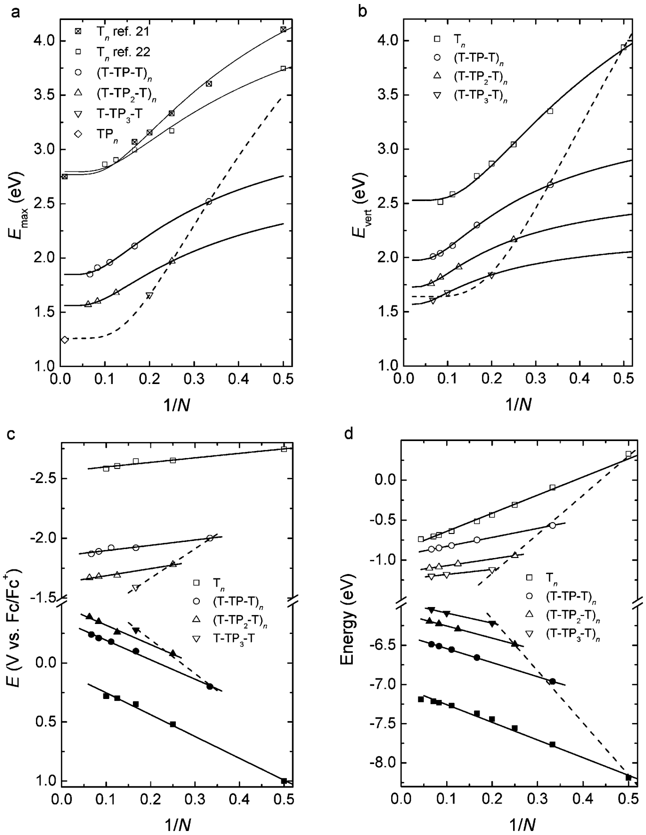

Figure 4. Experimental and calculated optical and electrochemical data for T_n, $(T-TP-T)_n$, $(T-TP_2-T)_n$, $(T-TP_3-T)_n$, and TP_n versus the inverse number of aromatic units. (a) Experimental E_{max}. (b) Calculated E_{vert}. (c) Experimental E_{ox} (solid markers) and E_{red} (open markers). (d) Calculated HOMO (solid markers) and LUMO (open markers) levels. Experimental data for T_n are from refs 21 and 22, for $(T-TP-T)_n$ from ref 8, for $T-TP_3-T$ from ref 9, and for TP_n from ref 5c. Lines in graphs a and b are according to eq 1, and those in graphs c and d assume a linear relation. The redox potentials are given as the onset of oxidation or reduction, except for the T_n series, where E^0 was taken for the oxidation potential and the reduction potential was estimated by subtracting E_{max} from this value.

of the curves of the HOMO−LUMO gap and E_{max}, when the thienopyrazine segment size increases. The absence of clear donor−acceptor character in these thienopyrazine oligomers originates from the fact that, according to the calculations, the thienopyrazine units are both a better electron acceptor *and* a better electron donor than thiophenes. This contrasts other more classical acceptor systems, like thiophene-*S*,*S*-dioxide, where mainly the LUMO levels are influenced by changing the acceptor content and donor character is absent.[23] The donor character of thienopyrazine increases the delocalization of the HOMO and increases the chain length dependence of the band gap and E_{max}.[3b] In fact, the delocalization of the HOMO level in T−TP systems is helpful because otherwise there would be, within a one-electron picture, no transition dipole moment between HOMO(D) and LUMO(A) and hence no significant absorption at low energy.

Figure 4c,d shows that for a fixed number of repeat units ($N = n + m$), the oxidation potential of a T_n-TP_m oligomer decreases when n decreases in favor of m. The lowering of the oxidation potential with increasing number of TP units implies that the T−TP systems are per se not “real” DA systems. For a DA system the HOMO of D should be well above that of A. We have calculated the frontier orbital levels of the T and TP monomers and of the T−T, T−TP, and TP−TP dimers (Figure 6). It can be seen that while the concept works for the LUMO, it completely fails for the HOMO, due to the fact that the HOMO of T is lower than that of TP. Hence, T−TP has a lower HOMO than TP−TP and it is not a real DA pair. Hence, TP is a better donor and acceptor than T, and by admixing TP in the polymer, the lowest band gap is found for pure poly-TP and not for a mixed T_n-TP_m compound.

To explain the low band gap with increasing TP fraction, admixing of quinoid character into the ground state can be considered.[3c] By adding more thienopyrazine units, the quinoid character may increase and the band gap would decrease to ultimately reach the value for poly(thieno[3,4-*b*]pyrazine). We note that the band gap for poly(thieno[3,4-*b*]pyrazine) is lower than for any of the mixed thiophene−thienopyrazine systems and that poly(thieno[3,4-*b*]pyrazine) and related compounds like poly(isothianaphthene) are known to possess a quinoid ground state.[24]

To investigate the possibility of quinoid character in the oligomers upon adding thienopyrazine units to the acceptor block, we compared the calculated bond length alternation in $T-TP_3-T$ with the bond length alternation calculated for quinquethiophene (5T). The data are depicted in Figure 7. From this graph, it can be seen that the bond length alternation inside the rings is around the value for 5T. The bond length alternation in the connecting bonds in $T-TP_3-T$, however, is about half the value of 5T. If a quinoid resonance form would be the reason for the band gap reduction in these systems, both inter-ring bond length alternation and the alternation within the rings would be reduced, which is clearly not the case here. Hence, although the inter-ring bonds do indicate some admixing of quinoid character to $T-TP_3-T$, the bond length alternation is not necessarily quinoid. The strong reduction of the inter-ring bond lengths indicates a stronger interaction and bonding between the thienopyrazine moieties than between the thiophene rings. All together, the theoretical results demonstrate that the introduction of extra thienopyrazine rings does not induce significant geometric distortions, thus suggesting that the acceptor segments are too short to accommodate a fully developed quinoid structure. This is further supported by the fact that the lowest optical transition of a model oligothiophene segment, where the BLA pattern characteristic of the $(T-TP_2-T)_n$ polymer was imposed, is only reduced by 0.06 eV compared to a regular oligothiophene.

The result that the interaction between neighboring thienopyrazine rings is more important than simple donor−acceptor effects is also supported by the electrochemistry data, depicted in Figure 4b, and the calculated HOMO and LUMO levels for the different series, depicted in Figure 4c. From these graphs it is clear that, for all series investigated (no, one, two, or three thienopyrazine units used as acceptor block), the chain length dependence is almost the same, the reduction of the band gap largely being caused by a rise of the HOMO level (reflected in a lowering of the oxidation potential) and to a lesser extent by a lowering of the LUMO level (lower reduction potential). The similar evolution and reduction of the oxidation potential in all series point to a delocalization of the HOMO over the entire molecule, also in the systems with high acceptor content, as supported by the theoretical calculations. This leads again to the conclusion that the donor character of the thienopyrazine moiety is important. At the same time, increasing the amount of thienopyrazine units in the repeating unit leads to an almost equal change in the oxidation and reduction potentials, meaning that the lowering of the LUMO level is accompanied

TABLE 4: Calculated Vertical Transition Energies (E_{vert}) and HOMO and LUMO Energies vs Vacuum for T_n, $(T-TP-T)_n$, $(T-TP_2-T)_n$, and $(T-TP_3-T)_n$

	T_n			$(T-TP-T)_n$			$(T-TP_2-T)_n$			$(T-TP_3-T)_n$		
n	E_{vert} (eV)	HOMO (eV)	LUMO	E_{vert} (eV)	HOMO (eV)	LUMO (eV)	E_{vert} (eV)	HOMO (eV)	LUMO (eV)	E_{vert} (eV)	HOMO (eV)	LUMO (eV)
1				2.67	−6.96	−0.57	2.17	−6.49	−0.94	1.84	−6.22	−1.12
2	3.94	−9.29	1.38	2.30	−6.66	−0.75	1.91	−6.30	−1.05	1.68	−6.09	−1.18
3	3.35	−8.19	0.33	2.11	−6.56	−0.82	1.82	−6.23	−1.09	1.61	−6.05	−1.20
4	3.04	−7.77	−0.09	2.04	−6.51	−0.85	1.76	−6.20	−1.10			
5	2.87	−7.56	−0.31	2.01	−6.49	−0.87						
6	2.75	−7.44	−0.44									
9	2.58	−7.37	−0.52									
12	2.51	−7.27	−0.64									
14	2.48	−7.22	−0.71									
23	2.43	−7.19	−0.74									

by a concomitant rise of the HOMO level. This is contradictory to expectations based on a simple donor−acceptor approach, where the HOMO is located mainly on the donor part of the molecule and increasing the number of thienopyrazines would mainly affect the LUMO, leaving the HOMO unaltered.

Conclusions

A homologous series of well-defined, small band gap $(T-TP_2-T)_n$ oligomers containing alternating blocks of two thiophene and two double thienopyrazine units has been prepared. The optical and electrochemical band gaps decrease with increasing chain length, leading to an extrapolated value of ~1.25 eV for the polymer. The absorption spectra of the triplet state and radical cations of these oligomers have been investigated by photoinduced absorption spectroscopy using triplet sensitization and electron transfer employing excitation of a fullerene derivative (PCBM) in toluene and benzonitrile, respectively. The $T_n \leftarrow T_1$ absorptions shift to lower energy when going from dimer to tetramer, thereby showing the same trend as the $S_1 \leftarrow S_0$ absorption. In the more polar benzonitrile, electron transfer rather than energy transfer takes place, yielding the radical cation of the oligomers, as expected on the basis of calculations. Again, the optical transitions shift to lower energy as the oligomer length increases.

Comparison of the optical and electrochemical data with E_{max} and redox potentials of closely related T_n, $(T-TP-T)_n$, and $T-TP_3-T$, as well as the calculated E_{vert} and frontier orbital levels for the different series, leads to the conclusion that, in these thiophene−thienopyrazine systems, the reduction of the band gap cannot be explained by simple donor−acceptor effects because the conjugation length dependence of E_{max} and the redox potentials for simple oligothiophenes and systems with one or two thienopyrazine units per repeating unit are all rather similar when plotted versus $1/N$. In these conjugated chains, the thienopyrazine unit is in fact rather electron-rich (poly-TP has a lower oxidation potential than poly-T; see Figure 4d) and has a tendency to provide the chain with a small quinoid-like character. The reduction of the band gap in polymers consisting of alternating thiophene and thienopyrazine blocks must therefore be attributed to the pronounced donor *and* acceptor character of thienopyrazine units and the strong interactions between neighboring thienopyrazine units, possibly with some admixing of quinoid character to the ground state.

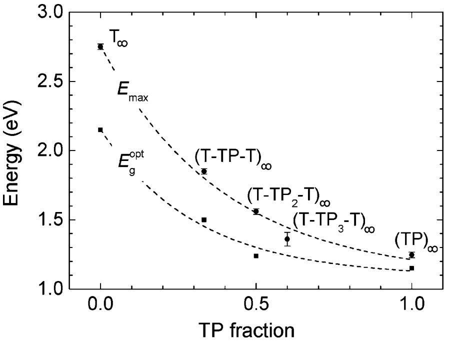

Figure 5. Experimental (T_n and TP_n) and extrapolated $(T-TP_x-T)_n$ values of E_{max} and E_g^{opt} for the polymers ($n = \infty$) versus the TP fraction in the chain. The value of $(T-TP_3-T)_\infty$ was estimated from the five-ring oligomer and extrapolating to $n = \infty$, using the chain length dependence found for $(T-TP_2-T)_n$ in Figure 4a.

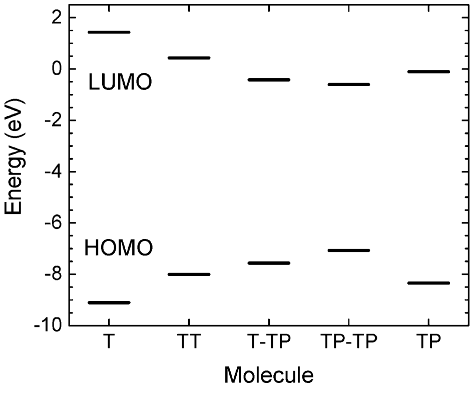

Figure 6. Calculated HOMO and LUMO levels of the monomers (T, TP) and dimers (T−T, T−TP, TP−TP).

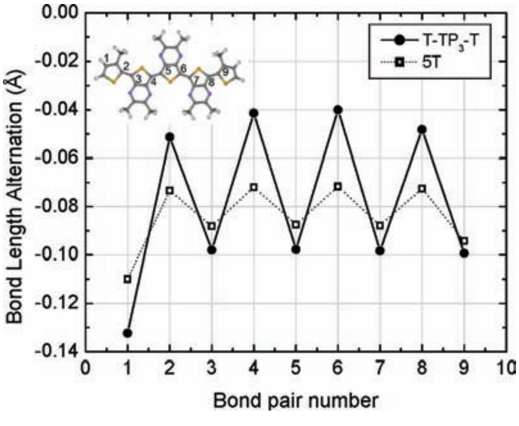

Figure 7. Calculated bond length alternation for $T-TP_3-T$ and 5T. The even bond pair numbers describe the bond length difference between the single bond that connects two thiophene rings with a double bond. The odd bond pair numbers describe the bond length difference between a single and double bond in a ring.

Acknowledgment. The research was supported by a TOP grant of the Chemical Sciences (CW) division of The Netherlands Organization for Scientific Research (NWO) and is part of the Joint Solar Programme (JSP). The JSP is cofinanced by the Foundation for Fundamental Research on Matter (FOM), Chemical Sciences of NWO, and the Foundation Shell Research. The joint collaboration is supported by the European Commission through the Human Potential Program Marie-Curie Research Training Network NANOMATCH (Grant No. MRTN-CT-2006-035884). The work in Mons is further supported by the Belgian National Fund for Scientific Research (FNRS). J.C. is a research fellow of FNRS. J.G. is a "Ramón y Cajal" research fellow, financed by the Spanish Ministry for Science and Innovation.

References and Notes

(1) (a) Dhanabalan, A.; Van Duren, J. K. J.; Van Hal, P. A.; Van Dongen, J. L. J.; Janssen, R. A. J. *Adv. Funct. Mater.* **2001**, *11*, 255–262. (b) Wang, X. J.; Perzon, E.; Delgado, J. L.; de la Cruz, P.; Zhang, F.; Langa, F.; Andersson, M.; Inganäs, O. *Appl. Phys. Lett.* **2004**, *85*, 5081–5083. (c) Campos, L. M.; Tontcheva, A.; Gunes, S.; Sonmez, G.; Neugebauer, H.; Sariciftci, N. S.; Wudl, F. *Chem. Mater.* **2005**, *17*, 4031–4033. (d) Wienk, M. M.; Turbiez, M. G. R.; Struijk, M. P.; Fonrodona, M.; Janssen, R. A. J. *Appl. Phys. Lett.* **2006**, *88*, 153511. (e) Admassie, S.; Inganäs, O.; Mammo, W.; Perzon, E.; Andersson, M. R. *Synth. Met.* **2006**, *156*, 614–623. (f) Zhang, F.; Mammo, W.; Andersson, L. M.; Admassie, S.; Andersson, M. R.; Inganäs, O. *Adv. Mater.* **2006**, *18*, 2169–2173. (g) Muhlbacher, D.; Scharber, M.; Morana, M.; Zhu, Z. G.; Waller, D.; Gaudiana, R.; Brabec, C. *Adv. Mater.* **2006**, *18*, 2884–2889. (h) Zhu, Y.; Champion, R. D.; Jenekhe, S. A. *Macromolecules* **2006**, *39*, 8712–8719. (i) Peet, J.; Kim, J. Y.; Coates, N. E.; Ma, W. L.; Moses, D.; Heeger, A. J.; Bazan, G. C. *Nat. Mater.* **2007**, *6*, 497–500. (j) Perzon, E.; Zhang, F.; Andersson, M.; Mammo, W.; Inganäs, O.; Andersson, M. R. *Adv. Mater.* **2007**, *19*, 3308–3311. (k) Bundgaard, E.; Krebs, F. C. *Sol. Energy Mater. Sol. Cells* **2007**, *91*, 954–985. (l) Wienk, M. M.; Turbiez, M.; Gilot, J.; Janssen, R. A. J. *Adv. Mater.* **2008**, *20*, 2556–2560.

(2) Scharber, M. C.; Muehlbacher, D.; Koppe, M.; Denk, P.; Waldauf, C.; Heeger, A. J.; Brabec, C. J. *Adv. Mater.* **2006**, *18*, 789–794.

(3) For reviews see: (a) Roncali, J. *Chem. Rev.* **1997**, *97*, 173–205. (b) Van Mullekom, H. A. M.; Vekemans, J. A. J. M.; Havinga, E. E.; Meijer, E. W. *Mater. Sci. Eng., R: Rep.* **2001**, *R32*, 1–40. (c) Kertesz, M.; Choi, C. H.; Yang, S. *Chem. Rev.* **2005**, *105*, 3448–3481. (d) Rasmussen, S. C.; Pomerantz, M. *Handbook of Conducting Polymers*, 3rd ed.; CRC: Boca Raton, FL, 2007.

(4) (a) Wudl, F.; Kobayashi, M.; Heeger, A. J. *J. Org. Chem.* **1984**, *49*, 3382–3384. (b) Kobayashi, M.; Colaneri, N.; Boysel, M.; Wudl, F.; Heeger, A. J. *J. Chem. Phys.* **1985**, *82*, 5717–5723. (c) Hoogmartens, I.; Adriaensens, P.; Vanderzande, D.; Gelan, J.; Quattrocchi, C.; Lazzaroni, R.; Brédas, J. L. *Macromolecules* **1992**, *25*, 7347–7356.

(5) (a) Pomerantz, M.; Chaloner-Gill, B.; Harding, L. O.; Tseng, J. J.; Pomerantz, W. J. *J. Chem. Soc., Chem. Commun.* **1992**, 1672–1673. (b) Nietfeld, J. P.; Heth, C. L.; Rasmussen, S. C. *Chem. Commun.* **2008**, 981–983. (c) Wen, L.; Duck, B. C.; Dastoor, P. C.; Rasmussen, S. C. *Macromolecules* **2008**, *41*, 4576–4578.

(6) (a) Havinga, E. E.; Ten Hoeve, W.; Wynberg, H. *Polym. Bull.* **1992**, *29*, 119–126. (b) Havinga, E. E.; ten Hoeve, W.; Wynberg, H. *Synth. Met.* **1993**, *55*, 299–306.

(7) Kitamura, C.; Tanaka, S.; Yamashita, Y. *Chem. Mater.* **1996**, *8*, 570–578.

(8) Karsten, B. P.; Viani, L.; Gierschner, J.; Cornil, J.; Janssen, R. A. J. *J. Phys. Chem. A* **2008**, *112*, 10764–10773.

(9) Karsten, B. P.; Janssen, R. A. J. *Org. Lett.* **2008**, *10*, 3513–3516.

(10) *AMPAC 6.55*; Semichem: Shawnee, KS, 1997.

(11) Ridley, J.; Zerner, M. *Theor. Chim. Acta* **1973**, *32*, 111–134.

(12) Gierschner, J.; Cornil, J.; Egelhaaf, H. J. *Adv. Mater.* **2007**, *19*, 173–191.

(13) Yamamoto, T.; Morita, A.; Miyazaki, Y.; Maruyama, T.; Wakayama, H.; Zhou, Z.; Nakamura, Y.; Kanbara, T.; Sasaki, S.; Kubota, K. *Macromolecules* **1992**, *25*, 1214–1223.

(14) (a) Meier, H.; Stalmach, U.; Kolshorn, H. *Acta Polym.* **1997**, *48*, 379–384. (b) Rissler, J. *Chem. Phys. Lett.* **2004**, *395*, 92–96.

(15) Van Hal, P. A.; Beckers, E. H. A.; Peeters, E.; Apperloo, J. J.; Janssen, R. A. J. *Chem. Phys. Lett.* **2000**, *328*, 403–408.

(16) Janssen, R. A. J.; Hummelen, J. C.; Wudl, F. *J. Am. Chem. Soc.* **1995**, *117*, 544–545.

(17) Weller, A. *Z. Phys. Chem. Neue Folge* **1982**, *133*, 93–98.

(18) Kooistra, F. B.; Mihailetchi, V. D.; Popescu, L. M.; Kronholm, D.; Blom, P. W. M.; Hummelen, J. C. *Chem. Mater.* **2006**, *18*, 3068–3073.

(19) Williams, R. M.; Zwier, J. M.; Verhoeven, J. W. *J. Am. Chem. Soc.* **1995**, *117*, 4093–4099.

(20) Van Bolhuis, F.; Wynberg, H.; Havinga, E. E.; Meijer, E. W.; Staring, E. G. J. *Synth. Met.* **1989**, *30*, 381–389.

(21) Bidan, G.; De Nicola, A.; Ene, V.; Guillerez, S. *Chem. Mater.* **1998**, *10*, 1052–1058.

(22) Kirschbaum, T.; Azumi, R.; Mena-Osteritz, E.; Bäuerle, P. *New J. Chem.* **1999**, *23*, 241–250.

(23) (a) Barbarella, G.; Favaretto, L.; Sotgiu, G.; Zambianchi, M.; Antolini, L.; Pudova, O.; Bongini, A. *J. Org. Chem.* **1998**, *63*, 5497–5506. (b) Barbarella, G.; Favaretto, L.; Zambianchi, M.; Pudova, O.; Arbizzani, C.; Bongini, A.; Mastragostino, M. *Adv. Mater.* **1998**, *10*, 551–554.

(24) (a) Brédas, J. L.; Heeger, A. J.; Wudl, F. *J. Chem. Phys.* **1986**, *85*, 4673–4678. (b) Nayak, K.; Marynick, D. S. *Macromolecules* **1990**, *23*, 2237–2245. (c) Kastner, J.; Kuzmany, H.; Vegh, D.; Landl, M.; Cuff, L.; Kertesz, M. *Macromolecules* **1995**, *28*, 2922–2929. (d) Cuff, L.; Kertesz, M. *J. Chem. Phys.* **1997**, *106*, 5541–5553.

JP9050148